Three-dimensional model of the negative hydrogen ion in a strong, linearly polarized light field

E. A. Volkova, A. M. Popov, and O. V. Tikhonova

D. V. Skobeltsyn Scientific-Research Institute of Nuclear Physics, M. V. Lomonosov State University, 119899 Moscow, Russia

(Submitted 2 March 1995; resubmitted 28 April 1995)
Zh. Éksp. Teor. Fiz. **108**, 436–446 (August 1995)

An algorithm is constructed for solving the two-dimensional single-electron Schrödinger equation for a quantum system in the field of an electromagnetic wave. This algorithm is then used to study the dynamics of the negative hydrogen ion in a strong light field. It is shown that at field strengths greater that atomic, a stabilization effect is observed. Calculations for one-dimensional and three-dimensional models of photoionization of the negative hydrogen ion are compared. © *1995 American Institute of Physics.*

1. INTRODUCTION

Direct numerical integration of the time-dependent Schrödinger equation for a quantum system in the field of an electromagnetic wave in recent years has become one of the main methods of investigating elementary processes in intense light fields.[1,2] Unfortunately, the larger requirements of computer time allow one to investigate the dynamics of only the simplest systems in the shortest laser pulses, no longer than a few tens of femtoseconds. A common technique for speeding up the calculations is to employ the simplest possible model of the phenomenon, which is to say, one-dimensional. Such a model, without describing many of the features of actual experiments (as, for example, the photoelectron angular distribution in the case of photoionization, effects associated with the polarization of laser radiation, etc.), still allows one to consider the interaction of an atomic electron with an electromagnetic field under conditions in which none of the commonly used approximations is justified. The number of papers dedicated to the analysis of a real, three-dimensional atom in a laser field is still not large. Thus, References 3 and 4 numerically solved the two-dimensional time-dependent Schrödinger equation for a hydrogen atom in the field of a linearly polarized electromagnetic wave. References 5 and 6 numerically modeled the ionization of a hydrogen atom in the $1s$ and $2p$ states in a circularly polarized field. A three-dimensional model of above-threshold ionization of a hydrogen atom being acted upon by a laser pulse with linear or circular polarization was considered in Ref. 7. We may also note an effort to construct a single-electron potential for the valence electron of a xenon atom[8] and study the process of photoionization from the $5p$ subshell in the approximation in which all the remaining electrons are frozen.

In the present paper we will use direct numerical integration of the two-dimensional time-dependent Schrödinger equation to investigate the process of photodetachment of an electron from a negative hydrogen ion. We then compare calculations of the dynamics of ionization of H^- in the one- and three-dimensional approximations.

2. SINGLE-ELECTRON MODEL OF A NEGATIVE HYDROGEN ION

From the physical point of view, the correct description of negative ions requires solution of the Schrödinger equation as a many-body problem. Such an approach can practically never be realized analytically and is often associated with great difficulties in the numerical treatment of systems with more than two electrons. In this regard, attempts have been made to reduce the problem to a one-electron problem. However, the question of the possibility of applying the single-electron approximation for describing negative ions is complicated. Atoms of the inert gases do not form bound states with electrons, so there are no negative ions with one electron above a completely filled shell. The appearance of an "extra" electron in the valence shell of an atom strongly redistributes its electron density, and this must be taken into account in any description of the interaction potential of a neutral atom and an electron. In the case of a negative hydrogen ion, the results obtained in the numerical solution of the two-particle problem indicate the possibility of using the single-electron approximation. A two-electron spatial wave function of the negative hydrogen ion that partly describes correlation effects it the Chandrasekhar function:[9,10]

$$\psi(r_1,r_2)=N\left[\exp\left(\frac{-r_1}{a_1}-\frac{r_2}{a_2}\right)+\exp\left(\frac{-r_2}{a_1}-\frac{r_1}{a_2}\right)\right] \qquad (1)$$

($a_1\approx 0.97\ a_0$, $a_2\cong 3.53\ a_0$, where a_0 is the Bohr radius, and N is a normalization factor), which corresponds to a single bound state with ionization potential $I=0.75$ eV. The maximum electron densities of the first and second electrons, calculated on the basis of the given wave function, have significantly different positions. This reflects the much weaker coupling of one of the electrons with the nucleus and, consequently, the validity of the single-electron approximation. To describe the system under study, we can use various single-particle potentials, which to varying degree take account of correlation and polarization effects.

In the simplest case, the single-electron potential for the weakly bound electron in a negative hydrogen ion can be represented in the form of the interaction potential of this electron and the neutral hydrogen atom:

 1063-7761/95/080235-06$10.00

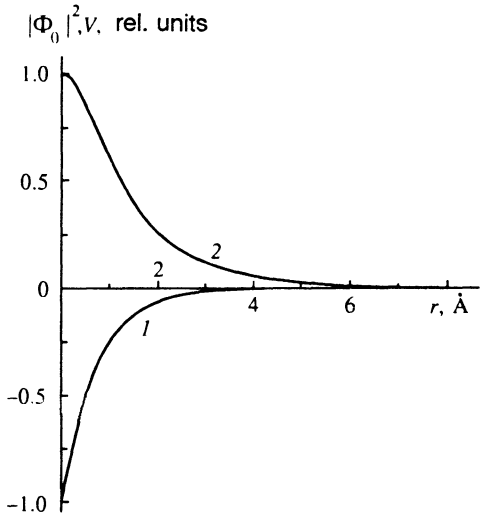

FIG. 1. 1) Single-electron potential and 2) radial distribution of the probability density $|\Phi_0(r)|^2$ for the ground state of the negative hydrogen atom.

$$V(r)=-\frac{e^2}{r}\left(1+\frac{r}{a}\right)\exp\left(-\frac{2r}{a}\right), \quad a=a_0. \tag{2}$$

However, it turns out that for such a potential it is not possible to form a discrete energy spectrum with the prescribed ionization potential ($I=0.75$ eV) and characteristic width of the electron density distribution for any value of a.

Therefore, we chose the potential created by the atomic shell for the outer electron in H^- in the form

$$V(r)=-\left(\frac{e^2}{\sqrt{\alpha^2+r^2}}+\frac{e^2}{\beta}\right)\exp\left(-\frac{2r}{\beta}\right), \tag{3}$$

where $\alpha=2.5a_0$ and $\beta=3a_0$.

This potential does not have a singularity at zero, as does the potential created by the hydrogen atom in empty space. In such a potential the electron has one bound state, characterized by the spherically symmetric function $\Phi_0(r)$ (see Fig. 1) and ionization potential $I\approx 0.75$ eV, which coincides with the experimental value for H^-. In this case, the width of the wave packet describing this state, $\Delta r=\sqrt{\langle r^2\rangle}$, is roughly equal to $2.5a_0$, which correspond to the half-width of the packet, Δx, describing the H^- ion in the one-dimensional model.[11] The coincidence of these parameters for the two models allows us to compare calculations of the dynamics of ionization using the one- and two-dimensional Schrödinger equations.

Note that the single-electron model of the negative hydrogen ion is valid for not-too-strong fields, i.e., for those fields that do not have an effect on the inner electron after passage of the laser pulse (i.e., fields that do not excite or ionize the inner subsystem). Corresponding estimates of the intensity of the electromagnetic field are made in Appendix A.

One should not expect the electron charge distribution for the given potential to coincide with the electron density obtained from the two-particle wave function, since for this it would be necessary to take the interaction of the electrons into account. But this, in its turn, would require a deeper analysis of the physical properties of the system, which would lead to a refinement of the single-electron potential.

3. NUMERICAL MODEL OF THE DYNAMICS OF AN H^- ION IN AN ELECTROMAGNETIC FIELD

In the dipole approximation in the appropriate cylindrical coordinate system the Schrödinger equation for the electron in the central potential $V(|\mathbf{r}|)$ in the presence of a linearly polarized electromagnetic wave is written in the form

$$i\hbar\frac{\partial\psi}{\partial t}=-\frac{\hbar^2}{2m}\left(\frac{1}{\rho}\frac{\partial}{\partial\rho}\rho\frac{\partial\psi}{\partial\rho}+\frac{\partial^2\psi}{\partial z^2}\right)+V(\rho,z)\psi$$
$$-ezE(t)\psi(\rho,z,t). \tag{4}$$

Here the z axis is aligned with the vector $\mathbf{E}$, and ρ is the radial coordinate of the electron $r=\sqrt{\rho^2+z^2}$.

We assume that initially the system is found in the unperturbed state of the atomic Hamiltonian

$$H_0=-\frac{\hbar^2}{2m}\nabla^2+V(\rho,z) \tag{5}$$

described by the wave function $\Phi_0(\sqrt{\rho^2+z^2})$.

The field of the electromagnetic wave was chosen in the form of a Gaussian pulse

$$E(t)=E_0\exp\left[-\frac{1}{2}\left(\frac{t-t_0}{\tau}\right)^2\right]\cos\omega t, \tag{6}$$

where $\tau_p=2\tau$ is the width of the pulse at half-maximum and t_0 is the time at which the laser intensity reaches its maximum value.

We calculated the ionization dynamics of a negative hydrogen atom for radiation with energy $\hbar\omega=5$ eV and pulse length $\tau_p=4$ fs. For these values the parameter $\tau_p/T\approx 5$ ($T=2\pi/\omega$ is the period of the field), i.e., the intensity of the radiation varies smoothly. The peak intensity of the radiation was varied from 10^{12} to $4\cdot10^{15}$ W/cm^2. The total integration time was $6\tau=12$ fs and was adequate to describe the ionization dynamics at the leading and trailing edges of the pulse.

The magnitude of the intensity corresponding to the atomic value of the field for the system under consideration $P_a\approx 3\cdot10^{13}$ W/cm^2, i.e., in the investigated range of parameters the intensities of the laser radiation were both greater than and less than the atomic value of the intensity.

In order to integrate it numerically, Eq. (4) was discretized on a 200×50 spatial grid in a region $120a_0\times30a_0$. The grid was chosen to be spatially nonuniform so as to more accurately describe the evolution of the wave function where the potential acts. Near the boundary of the calculated region ($z=\pm z_{\max}$, $\rho=\rho_{\max}$) an imaginary term was added to the potential which describes absorption of the probability density and eliminates reflection from the boundaries. More detailed information about the numerical solution technique is given in Appendix B.

4. MODEL RESULTS

Figure 2 presents the calculated evolution of the probability density $|\psi(\rho,z)|^2$ of detecting an electron at different

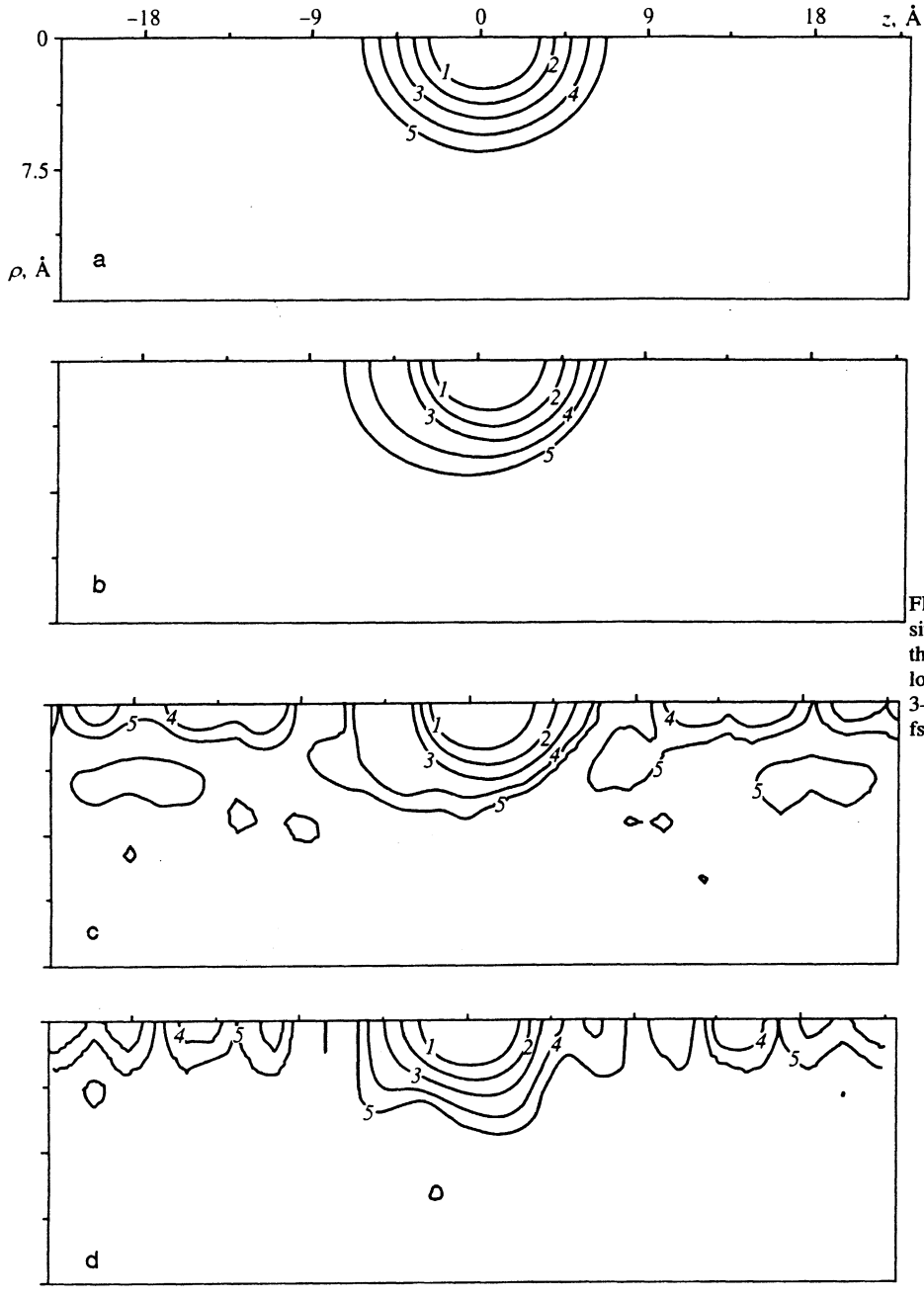

FIG. 2. Spatial distributions of the probability density $|\psi(\rho,z)|^2$ at different times during the action of the laser pulse. The contours correspond to the following values of $|\psi(\rho,z)|^2$: 1—10^{-2}, 2—$3\cdot10^{-3}$, 3—10^{-3}, 4—$3\cdot10^{-4}$, 5—10^{-4}. Times: a) 0, b) 3.2 fs, c) 6.4 fs, d) 11.2 fs.

points in space for a radiation intensity $P=2\cdot10^{13}$ W/cm^2. Figure 2a shows the initial wave function ($t=0$), Figs. 2b, c, and d correspond to the times 3.2, 6.4, and 11.2 fs, respectively. Figure 2c depicts the probability density distribution at the time when the radiation intensity is near maximum, while Fig. 2d shows it while the lasing decays, when the ionization process had already ceased. These distributions show that the electronic escapes primarily in the direction of the electric field of the wave, and that as the laser pulse passes a series of wave packets is formed, moving away from the potential well along the z axis in the positive and negative directions. This is because the electronic escapes from the atom preferentially at the time the electric field reaches its amplitude value, i.e., photodetachment of the electron resembles tunneling. Evaluation of the Keldysh parameter

$$\gamma=\frac{\omega\sqrt{2mI}}{eE_0}$$

for the given case actually gives $\gamma\approx1$. The spatial distributions of the electron density for various values of the laser intensity at the time roughly corresponding to the maximum intensity of the radiation are shown in Fig. 3. Note that in the intensity region $P=10^{14}-10^{15}$ W/cm^2 the ionization has an above-barrier character: the electron wave packet executes vibrational motion near its initial position, gradually delocalizing in space and scattering from the atomic potential. This picture is very similar to the dynamics of the ionization of a one-dimensional negative hydrogen ion, considered in Ref. 11.

In our calculation of the action of the laser pulse, we also calculated the probability $W(t)$ of detecting the electron in

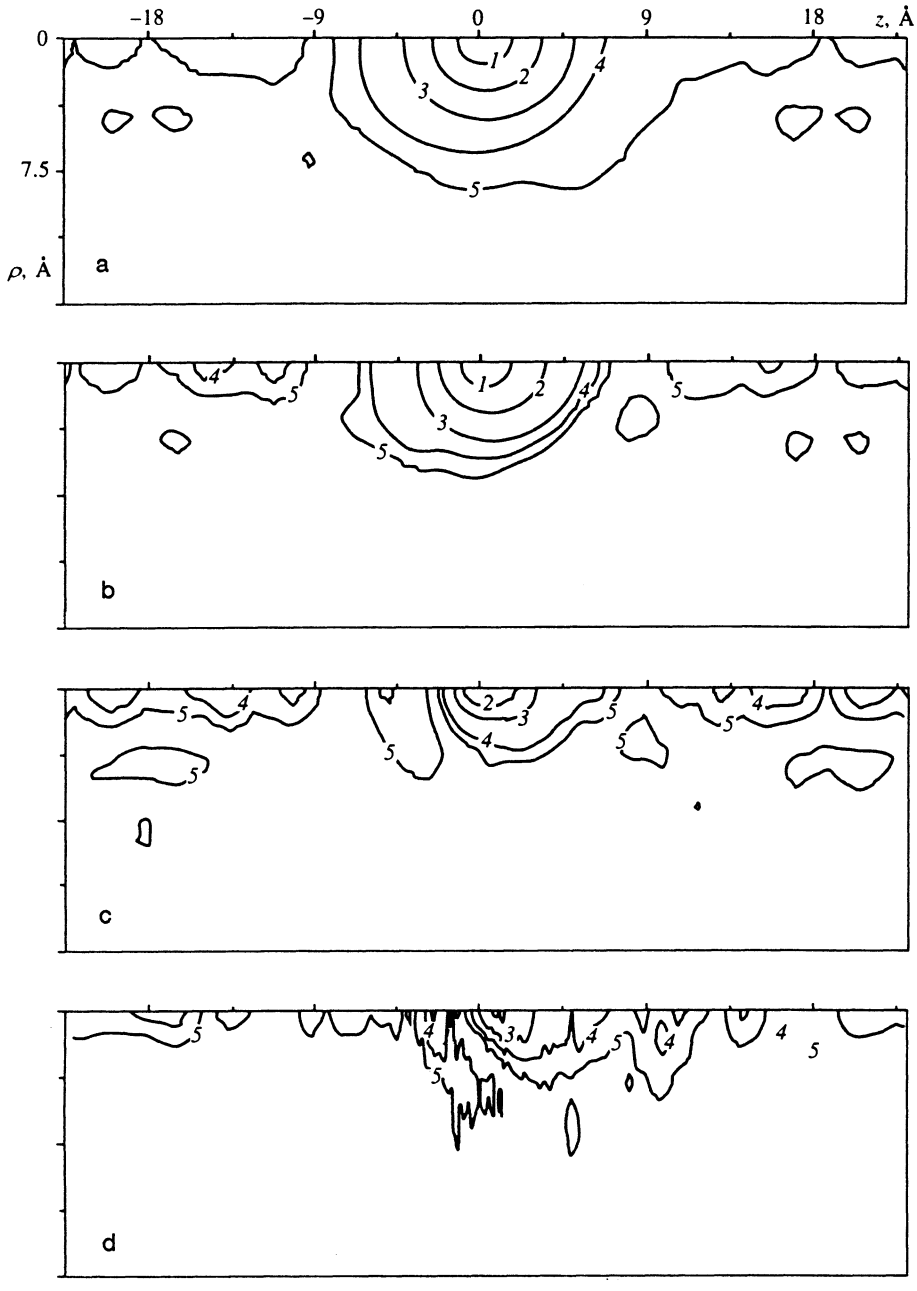

FIG. 3. Spatial distributions of the probability distribution $|\psi(\rho,z)|^2$ at the times of maximum radiation intensity (W/cm^2) for P equal to a) 10^{12}, b) 10^{13}, c) 10^{14}, d) 10^{15}. The contours correspond to the following values of $|\psi(\rho,z)|^2$: a) 1—0.1, 2—10^{-2} 3—10^{-3}, 4—10^{-4}, 5—10^{-5}; b) 1—0.1, 2—10^{-2}, 3—10^{-3}, 4—$3\cdot10^{-4}$, 5—10^{-4}; c,d) 2—10^{-2}, 3—$3\cdot10^{-3}$, 4—10^{-3}, 5—$3\cdot10^{-4}$.

its initial bound state. This probability is defined as the projection of the calculated wave function $\psi(\rho,z,t)$ onto the state $\Phi_0(\sqrt{\rho^2+z^2})$:

$$W(t)=\left|\int \psi^*(\rho,z,t)\Phi_0(\sqrt{\rho^2+z^2})2\pi\rho d\rho dz\right|^2. \qquad (7)$$

The functional dependence $W(t)$) is plotted in Fig. 4 for various values of the intensity. Note that these dependences are qualitatively similar to the results obtained in the one-dimensional calculations of Refs. 11 and 12. The most important feature of the ionization dynamics is the high-frequency oscillations (with twice the frequency of the laser radiation) of $W(t)$, for which the depth of modulation of the curve $W(t)$ grows rapidly as a function increase of the intensity (see Fig. 4). For the radiation intensity $P=4\cdot10^{15}$ W/cm^2 the probability W within one period of the optical wave varies over six orders of magnitude and qualitatively corresponds to the model of almost free oscillations of the

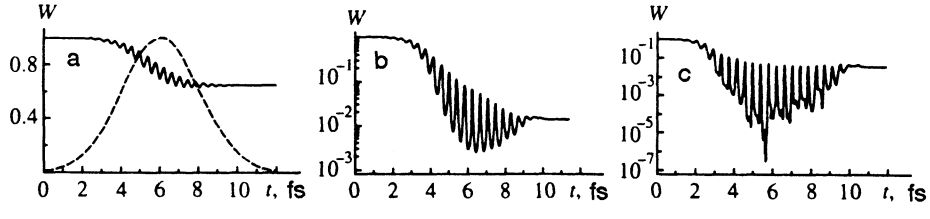

FIG. 4. Dynamics of the probability of detecting the system in its initial bound state for radiation intensities a) $2\cdot10^{13}$ W/cm^2, b) $5\cdot10^{14}$ W/cm^2, c) $4\cdot10^{15}$ W/cm^2; broken trace—envelope of the laser pulse.

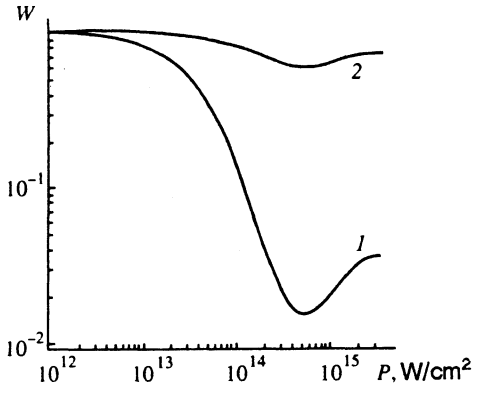

FIG. 5. Probability of detecting the system in its initial bound state as a function of radiation intensity: 1) two-dimensional calculation, 2) one-dimensional calculation.

electron wave packet proposed in Ref. 11. The authors of Refs. 11 and 12 noted that when the field of the electromagnetic wave exceeds the atomic field a stabilization effect should be observed, that is, the probability of ionization of the system by the laser pulse should decay with increase of the intensity of the pulse. The physical reasons for the stabilization phenomenon have been discussed repeatedly in the literature and expounded in detail in Refs. 1 and 13.

The probability of detecting the electron in the bound state after passage of the laser pulse, calculated in both the one-dimensional approximation (using the one-dimensional potential given in Ref. 11) and the three-dimensional approximation as a function of the intesntiy, is plotted in Fig. 5. It turns that the effect of ionization suppression in a strong field arises for both models, and the two models have the same threshold for suppression, $5\cdot10^{14}$ W/cm^2. The two models differ mainly in their probabilities of detecting the atom in the ground state after the passage of the laser pulse. For $P=5\cdot10^{14}$ W/cm^2 the difference in the probabilities is more than one and a half orders of magnitude. We suppose that the "lighter" ionization of the three-dimensional atom is connected with additional delocalization of the wave function in the direction perpendicular to the electric field vector of the wave and the resulting faster decay of the overlap integral (7) during the passage of the laser pulse. Reference 14 contains a comparison of the one- and three-dimensional models of the hydrogen atom in a strong electromagnetic field. This comparison revealed a great stability to ionization of the one-dimensional system. On the other hand, this effect implies that stabilization in the three-dimensional system is manifested more sharply: as the intensity rises from $5\cdot10^{14}$ W/cm^2 to $4\cdot10^{15}$ W/cm^2, the magnitude of W grows roughly threefold for the three-dimensional atom and only by about 10% for the one-dimensional atom.

Note, in conclusion, that the magnitude of the stabilization threshold of this system turns out to be roughly equal to the limit of the region of applicability of the single-electron approximation for H^-. Therefore, a study of the dynamics of the negative hydrogen ion in a superatomic field would require additional consideration, with attention given to the effect of the electromagnetic field of the wave on the inner electron.

ACKNOWLEDGMENTS

This work was supported by the International Science Fund (ISF), Project No. NCN000, the Russian Fund for Fundamental Research, Project No. 95-02-06258a, and also by a combined grant of the ISF and the Russian government, No. NCN300.

APPENDIX A: ESTIMATE OF THE INFLUENCE OF THE ELECTROMAGNETIC FIELD ON THE INNER ELECTRON IN A NEGATIVE HYDROGEN ION

In the present paper we investigate the interaction of the outer, weakly coupled electron of a negative hydrogen ion with an intense laser pulse of finite duration in the single-particle approximation. The single-electron approach is valid if the conditions of the interaction are such that it can be assumed that neither ionization nor excitation of the inner subsystem (hydrogen atom) takes place. It can then be assumed that this inner electron is found in the $1s$ state of the hydrogen atom. The lower limit of the field at which the single-electron approximation is no longer valid can be taken to be the field E_{cr} which noticeably populates the excited states of the hydrogen atom during the time of the pulse $\tau_p=2\tau$. The magnitude of this field was estimated from the transition probability in a two-level system. Here we assumed adiabatic turning on of the field, since the condition $\tau_p/T\gg1$ is fulfilled under the conditions of our problem. The probability of population of the $2p$ (excited) level under these conditions has the form:[13]

$$W_{2p}=\frac{1}{2}\left(1-\frac{|\Delta|}{2\Omega}\right),$$

where Δ is the detuning and Ω is the Rabi frequency.

Taking as critical a field that leads to 5% population of the upper level, we obtain the following estimate for the critical intensity:

$$P_{cr}=cE_{cr}^2/8\pi\approx5.5\cdot10^{14}\ \text{W/cm}^2.$$

APPENDIX B: METHOD OF NUMERICAL INTEGRATION OF THE TWO-DIMENSIONAL TIME-DEPENDENT SCHRÖDINGER EQUATION

To solve Eq. (4), we used the method of splitting the equation according to physical factors, described in Ref. 15. In this approach, Eq. (4) is first discretized in time with time step Δt. In this way, Eq. (4) is replaced by a chain of equations describing the spreading of the wave function in space and its behavior in the total field of the potential and the electromagnetic wave. The wave equations in the field is an ordinary differential equation, and is solved in the same way as in Ref. 15.

Let us mention the solution of the equation describing the spreading of the wave function

$$i\hbar\frac{\partial\psi}{\partial t}=-\frac{\hbar^2}{2m}\left(\frac{1}{\rho}\frac{\partial}{\partial\rho}\rho\frac{\partial\psi}{\partial\rho}+\frac{\partial^2\psi}{\partial z^2}\right). \tag{8}$$

We discretize Eq. (B1) in the spatial variables by using finite elements with cubic interpolation of the function at each element. As a result, we obtain a system of ordinary differential equations for the vector of grid values of the wave function $\psi(t)=\{\psi_i(t)\}$. Here i is the index of the spatial grid point:[16]

$$\mathbf{M}_z\otimes\mathbf{M}_\rho\frac{d\psi}{dt}=\mathbf{M}_z\otimes\mathbf{D}_\rho\psi(t)+\mathbf{D}_z\otimes\mathbf{M}_\rho\psi(t),$$

$$(M_\rho)_{ij}=\int N_iN_j\rho d\rho,\quad (M_z)_{ij}=\int N_iN_jdz, \tag{9}$$

$$(D_\rho)_{ij}=-\frac{\hbar}{2m}\int N_iN_j\rho d\rho,\quad (D_z)_{ij}=\frac{\hbar}{2m}\int N_iN_jdz,$$

where $\mathbf{M}$ and $\mathbf{D}$ are the analogs of the weight matrix and the stiffness matrix, N_i is the cubic function of the form, and $\otimes$ is the direct product of the matrices.

The time derivative is approximated according to a semi-implicit scheme with implicitness parameter 0.5 (Crank–Nicolson scheme)

$$\mathbf{M}_z\otimes\mathbf{M}_\rho(\psi^{n+1}-\psi^n)=\frac{\Delta t}{2}(\mathbf{M}_z\otimes\mathbf{D}_\rho+\mathbf{D}_z\otimes\mathbf{M}_\rho)\times(\psi^{n+1}+\psi^n), \tag{10}$$

where ψ^{n+1} and ψ^n are the vector function ψ at the nth and $n+1$th time step.

This scheme is of order $(\Delta t^2,\Delta r^2,\mathbf{D}_z^2)$. To within terms of order $[(1/4)\Delta t^2\mathbf{D}_z\otimes\mathbf{D}_r\Delta\psi^{n+1}]$, Eq. (10) can be reduced to the form

$$\left(\mathbf{M}_z-\frac{1}{2}\mathbf{D}_z\right)\otimes\left(\mathbf{M}_\rho-\frac{1}{2}\mathbf{D}_\rho\right)\Delta\psi^{n+1}=R^n\Delta t,$$
$$\Delta\psi^{n+1}=\psi^{n+1}-\psi^n, \tag{11}$$

where R^n is a vector to be determined by the function at the nth time step.

Equation (11) can be split into two equations corresponding to the one-dimensional problems

$$\left(\mathbf{M}_z-\frac{1}{2}\mathbf{D}_z\right)\Delta\psi^*=R^n\Delta t, \tag{12a}$$

$$\left(\mathbf{M}_\rho-\frac{1}{2}\mathbf{D}_\rho\right)\Delta\psi^{n+1}=\Delta\psi^*. \tag{12b}$$

Let the number of grid points in z be K_z, and in r be K_r. Then Eq. (12a) consists of K_r scalar equations in a vector of dimensionality K_z, and Eq. (12b) consists of K_z scalar equations in a vector of dimensionality K_r.

The one-dimensional equations of system (12) were solved by LDL-factorization,[17] in which the matrix on the left side of the equation is split into an upper and a lower triangular matrix and a diagonal matrix.

This work was supported by the International Science Foundation (Project No. NCN000) Russian Fund for Fundamental Research (Project No. 95-02-06258a), and also by the Joint Grant No. NCN300 of the International Science Foundation and the Russian Government.

[1] N. B. Delone and V. P. Krainov, *Multiphonon Processes in Atoms* (Springer-Verlag, New York, 1993).
[2] A. M. Popov and E. A. Volkova, Laser Phys. **5** (in press).
[3] K. C. Kulander, Phys. Rev. A **35**, 445 (1987).
[4] K. C. Kulander, K. J. Schafer, and J. L. Krause, Phys. Rev. Lett. **66**, 2601 (1991).
[5] M. Pont and M. Gavrila, Phys. Rev. Lett. **65**, 2362 (1990).
[6] M. Gajda, B. Piraux, and K. Rzążewski, Phys. Rev. A **50**, 2528 (1994).
[7] R. A. Blank and M. Shapiro, Phys. Rev. A **50**, 3234 (1994).
[8] K. C. Kulander, Phys. Rev. A **38**, 778 (1988).
[9] H. A. Bethe and E. E. Salpeter, *Quantum Mechanics of One- and Two-Electron Atoms* (Springer, Berlin, 1957).
[10] B. M. Smirnov, *Negative Ions* (McGraw-Hill, New York, 1982).
[11] R. Grobe and M. V. Fedorov, Laser Phys. **3**, 265 (1993).
[12] E. A. Volkova and A. M. Popov, Zh. Éksp. Teor. Fiz. **105**, 592 (1994) [JETP **78**, 315 (1994)].
[13] N. B. Delone and V. P. Kraniĭnov, *Atoms in Strong Light Fields* (Springer-Verlag, New York, 1985).
[14] T. Millack, J. Phys. B **26**, 4777 (1993).
[15] E. A. Volkova, A. M. Popov, and O. B. Popovicheva, Zh. Éksp. Teor. Fiz. **102**, 496 (1992) [Sov. Phys. JETP **75**, 263 (1992)].
[16] C. A. Fletcher, *Computational Galerkin Methods* (Springer-Verlag, New York, 1983).
[17] D. H. Norrie and G. de Vries, *The Finite Element Method: Fundamentals and Applications*, Academic, New York (1973).

Translated by Paul F. Schippnick